31st Annual International Conference of the IEEE EMBS
Minneapolis, Minnesota, USA, September 2-6, 2009

Distribution of traction forces associated with shape changes during amoeboid cell migration

B. Alonso-Latorre[1], R. Meili[2], E. Bastounis[1], J. C. del Álamo[1], R. Firtel[2] and J. C. Lasheras[1]

***Abstract*—Amoeboid motility results from the cyclic repetition of shape changes leading to periodic oscillations of the cell length (*motility cycle*). We analyze the dominant modes of shape change and their association to the traction forces exerted on the substrate using Principal Component Analysis (PCA) of time-lapse measurements of cell shape and traction forces in migrating *Dictyostelium* cells. Using wild-type cells (*wt*) as reference, we investigated Myosin II activity by studying Myosin II heavy chain null cells (*mhcA*-) and Myosin II essential light chain null cells (*mlcE*-). We found that *wt, mlcE*- and *mhcA*- cells utilize similar modes of shape changes during their motility cycle, although these shape changes are implemented at a slower pace in Myosin II null mutants. The number of dominant modes of shape changes is surprisingly few with only four modes accounting for 75% of the variance in all cases. The three principal shape modes are dilation/elongation, bending, and bulging of the front/back. The second mode, resulting from sideways protrusion/retraction, is associated to lateral asymmetries in the cell traction forces, and is significantly less important in *mhcA*- cells. These results indicate that the mechanical cycle of traction stresses and cell shape changes remains remarkably similar for all cell lines but is slowed down when myosin function is lost, probably due to a reduced control on the spatial organization of the traction stresses.**

Keywords: cell motility, cell migration, traction stresses, actin polymerization, principal component analysis, dictyostelium

I. Introduction

Amoeboid motility plays an important role in many physiological processes such as embryonic development, tissue renewal and the functioning of the immune system. It is also very important in pathological processes such as the metastasis of some cancers [2]. Several types of external stimuli may trigger directed cell motion. This process is controlled by a complex network of signaling biochemical pathways, which continuously drive the remodeling of the cytoskeleton of the cell and its adhesions to the extracellular matrix (ECM). Despite the complexity of the underlying biochemical pathways, the mechanical implementation of cell motility consists of a relatively simple cyclic succession of mechanical events: leading-edge protrusions, formation of new adhesions near the front, cell contraction, release of the adhesions and retraction from the rear [1] (Figure 1).

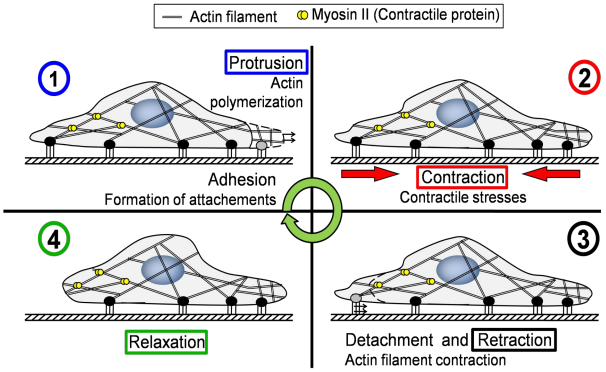

Fig. 1. Illustration of the different stages of the *motility cycle* of an amoeboid cell, adapted from [1].

Both leukocytes and *Dyctiostelium discoideum* in amoeboid form exhibit the above *motility cycle* with successive extension and retraction of pseudopods resulting in periodic temporal oscillations of the cell's length [3, 4], as well as the traction forces transmitted to the substrate [4-6].

Despite an increasingly detailed knowledge of the biochemistry of the cytoskeleton and the pathways that regulate its remodeling during migration, a better understanding of the spatiotemporal integration of these biochemical processes into specific events during cell migration is still needed. In particular, the precise mechanisms whereby each stage of the motility cycle is related to specific biochemical signaling events are not yet clear.

Our approach consists of using mechanical readouts such as cell shape and the distribution of traction forces to analyze how they change in response to changes in biochemical properties of the cell. For this purpose, we apply Principal Component Analysis (PCA) to high-resolution time-lapse simultaneous recordings of the shape and traction forces in wild type *Dyctiostelium discoideum* amoeboid cells as well as various mutants with adhesion or contractility defects.

II. Quantitative Evidence of a Force Regulated Motility Cycle

Amoeboid cells migrate undergoing a limited set of shape changes that compose the *motility cycle*: protrusion of the front through actin polymerization, attachment to the substrate, contraction of the cell body, followed by the detachment and retraction of the posterior part of the cell.

Manuscript received April 7, 2009. This work was supported in part by 1R01 HL0805518 NIH , BRP081804F NIH.

Baldomero Alonso-Latorre, Juan Carlos del Álamo, Effie Bastounis and Juan C. Lasheras are in the Departments of Mechanical and Aerospace Engineering and Bioengineering at the University of California, San Diego. La Jolla CA 92093-0411. (Corresponding author: lasheras@ucsd.edu).

Ruedi Meili and Richard Firtel are in the Department of Cell and Developmental Biology. University of California, San Diego. La Jolla CA 92093

This series of steps results in variations of the cell length: during protrusion the cell length increases and during retraction it decreases. In addition, the strain energy exerted by the cell on the elastic substrate also varies periodically in phase with the cell length (Figure 2 a-b). The existence of a biochemically coordinated *motility cycle* is demonstrated in both the auto and cross correlation of cell length (L) and strain energy (U_s) shown in Figure 2a-b for a typical *wt* cell. Observe that both L and U_s fluctuate in a cyclic fashion and are highly correlated. The autocorrelation of U_s, R_{UsUs}, and the cross-correlation between L and U_s, R_{LUs}, also show a marked degree of periodicity. The period of the motility cycle, T, is determined as the time lapse between peaks. The magnitude of the peaks for both R_{UsUs} and R_{LUs} is sustained over a long period of time indicating that (1) the variations in the cell length and stresses, are cyclic, and that (2) the cell length is positively correlated with the cell stresses. Similar results are obtained when examining *mhcA*- and *mlcE*- cells. In fact, the probability density functions of the correlation coefficient between U_s and L, r_{LUs}, for all the three cell lines under study, shown in Figure 2c, indicate that they are strongly correlated in all our experiments. The percentage of cells showing a correlation coefficient r_{UsL} larger than 0.5 is 33% for *wt*, 49% for *mhcA*- and 55% for *mlcE*-.

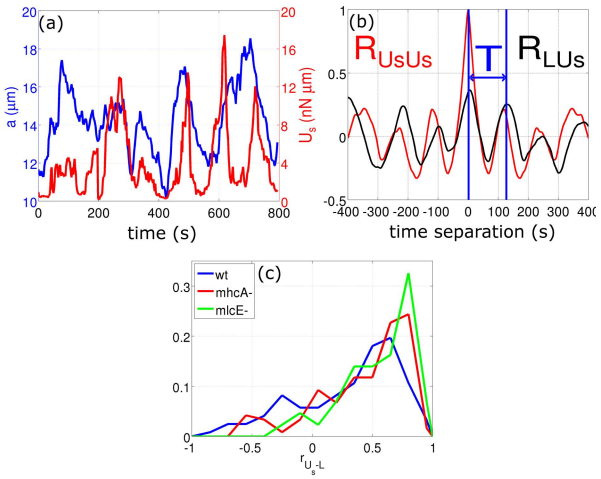

Figure 2. (a) Example of the temporal evolution of the major cell semiaxis, a (blue) and the strain energy, U_s (red) for a *wt* cell. The strain enegy, U_s, represents the work the cell needs to exert to deform the substrate. (b) Auto-correlation of the strain energy, R_{UsUs} (red); and cross-correlation between cell length and strain energy, R_{LUs} (black); as a function of the time separation. (c) Histogram of the correlation coefficient between the strain energy U_s and the length of the cell L for *wt* (blue, N=31 cells), *mhcA*- (red, N=27 cells) and *mlcE*- (green, N=14 cells) cells.

III. The Velocity of Migration is Determined by the Period of the Motility Cycle

Measurements on a large number of cells (N=86) have shown that the velocity of *Dictyostelium* cells chemotaxing on flat surfaces is determined by the rate at which the cells are able to repeat their *motility cycle* (Figure 3). The relationship between the average migration velocity of a cell (V) and the period of its strain energy cycle (T) is well approximated by the hyperbola $VT=L_0$, where L_0 is a constant with units of length [4]. Figure 3 also presents data from *talin A null* cells, a mutant with adhesion defects. Despite the reduced traction forces reported for these cells [4], they lay on the same hyperbola, with velocities and periods comparable to *wt* cells.

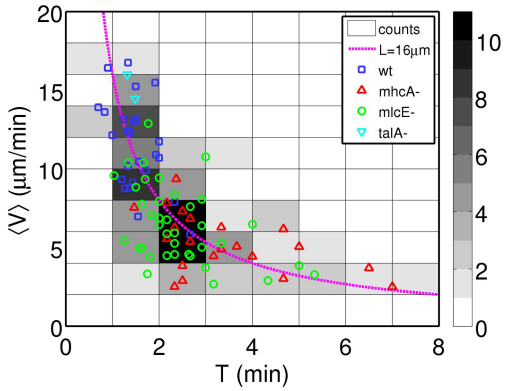

Figure 3. Scatter plot of the average velocity of N = 86 chemotaxing *Dictyostelium* cells versus the period of their motility cycle. The data points come from five different cell lines: N = 25 *wt* cells (blue squares), N = 21 *mhcA*- cells (red triangles), N = 38 *mlcE*- cells (green circles), and N = 2 *talA*- cells (cyan triangles). The dashed magenta hyperbola ($V = L/T$) is a least square fit to the data, yielding $L=15.7\ \mu m$. The $V-T$ plane has been divided into tiles that have been colored according to the number of cells whose speed and motility period lie within each tile. Darker tiles contain more cells, as indicated in the color. The correlation coefficient between V and $1/T$ is 0.71 ($p=10^{-14}$).

The correlation coefficient between V and $1/T$ is $R=0.71$ ($p=10^{-14}$). The fact that, regardless of the speed of migration, a cell advances on the average a fixed length per cycle suggests that although there are many interconnected molecular regulatory loops, the complex mechano-chemical system must settle into a relatively simple quasi-periodic cycle.

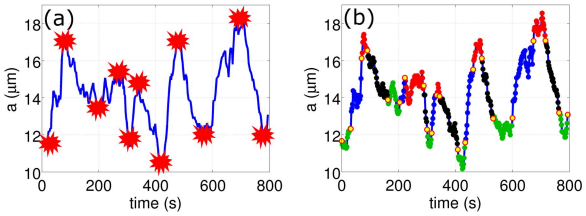

Figure 4. Representation of the steps of the algorithm used to calculate the phase averages. (a) After the major semiaxis of the cell, $a(t)$, is recorded for every frame, the peaks and valleys of each time history are identified. Panel (a) shows the time evolution of the semiaxis of a *wt* cell (blue line) and the determined location of the peaks and valleys of that time evolution. Panel (b) shows the output of the algorithm for the automatic dissection of the *motility cycle* into stages: protrusion (blue), contraction (red), retraction (black) and relaxation (green).

IV. Phase Average Analysis of the Motility Cycle

The biochemical and mechanical organization of the cell in space and time during the migration cycle can be analyzed by dividing the *motility cycle* into a number of canonical stages and then compiling the phase average maps of the shape and traction forces at each stage. For this purpose, we have developed an automatic procedure to identify these stages of the *motility cycle* in each experimental time-lapse

record (Figure 4). In addition, to compile average maps of traction forces coming from different cells at different instants of time, it is necessary to take into account the changes in shape and orientation of the cell that occur between measurements. This was achieved by using a cell-based reference system with its origin at the instantaneous location of the centroid and its horizontal axis coinciding with the orientation of the major moment of inertia of the cell [4].

V. Principal Component Analysis (PCA) of the Shape, Traction Force, and Chemical Intracellular Markers

In spite of its biochemical complexity, cell migration is the result of the quasi-periodic repetition of a reduced set of steps (and shape changes). Therefore, it is fundamental to identify not only the statistically significant shape changes, but also the biochemical and mechanical processes involved in the generation of each shape mode. For this purpose, we have implemented a statistical analysis called Principal Component Analysis (PCA) [7]. PCA enables us to identify for each cell line the most statistically-representative shape patterns that occur during the migration of a cell together with the weight factors (variance) that determine the relative contribution of each mode at each instant of time. We consider the shape of the cell as a two dimensional scalar field allowing us to relate it to the distributions of measured traction forces associated with each of the principal shape modes.

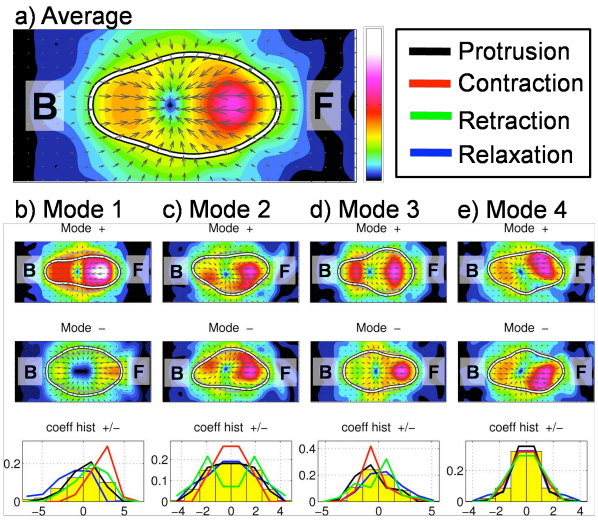

Figure 5. PCA of the shape and traction forces of a migrating *wt Dictyostelium* cell. (a): average shape and traction forces. The white contour indicates the contour of the cell. The color contours indicate the magnitude of the stresses and the arrows indicate their direction. (b)-(e): four most dominant shape modes patterns for positive (top) and negative (bottom) values of the weight factor. The bar plots in the lower panels show the distribution of instantaneous weight factors for this cell during the whole time history of the cell (yellow bars) and during each stage of the *motility cycle* (color curves). For all panels "F" is the front of the cell and "B" is the back of the cell.

The shape modes obtained from the PCA analysis are highly reproducible from cell to cell. Four out of the five most-representative shape mode patterns of each cell were common for all the cell lines studied. Furthermore, these four common, most representative modes in the PCA are enough to account for three quarters of the observed shape variance in migrating *Dictyostelium* cells (75% ± 4% for N = 23 *wt* cells, 75% ± 4% for N = 22 *mhcA*$^-$ cells and 76% ± 3% for N = 15 *mlcE*$^-$ cells). These results indicate that the dynamics of the shape changes in all migrating cells have a small number of degrees of freedom, in agreement with previous PCA of the cell contour performed in migrating *wt Dictyostelium* cells and keratocytes [8, 9]. Figure 5 shows the four most relevant shape mode patterns and their associated traction forces for a *wt* cell. The modes for *mhcA*- and *mlcE*- cells are similar (Figures 6 and 7). Figures 5-7 also contain histograms of the instantaneous values of the weight factors of each PCA mode. Positive/negative values of those weight factors correspond to the (+)/(-) configuration of each mode.

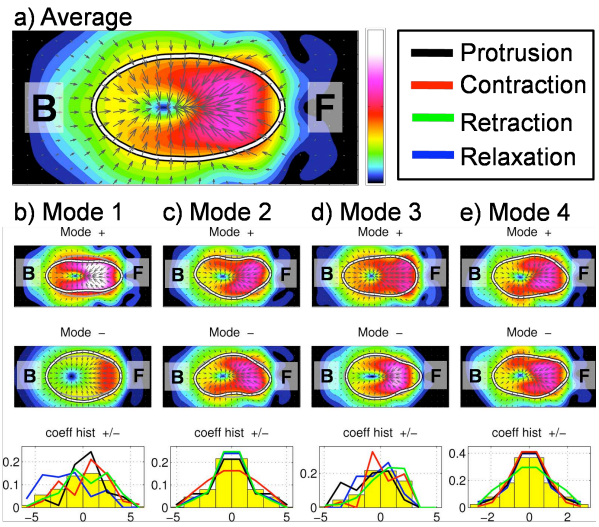

Figure 6. PCA of the shape and traction forces of a migrating *mhcA-Dictyostelium* cell.

The most important shape mode in terms of variance is Mode 1, which accounts for the changes in the aspect ratio of cell shape due to the periodic oscillations in cell length. As one would expect, the weight factors are predominantly positive during contraction, when the cell reaches its maximum length. Conversely, during relaxation, when the cell is roundest, the weight factors are predominantly negative. Note that the forces associated with the (+) shape pattern of Mode 1 (contraction phase) are high, whereas the forces associated with the (-) one (relaxation phase) are very low. Mode 2 is the second most statistically relevant shape mode. It is associated with the bending of the cell (a half-moon shape) and lateral asymmetries in the traction forces. This mode represents the events of lateral protrusion and retraction of pseudopods. Mode 3 represents a non-symmetric bulging and contraction of the front and back. It is important to notice that the relative contribution of the positive and negative modes differ between protrusion and retraction. The (-) mode is prominent during protrusion, when the cell is extending a frontal pseudopod and the (+) mode during retraction, when the cell is retracting its posterior part. The traction stresses associated to the (+) mode are higher in the front than in the back of the cell. In the (-) mode the increment of the force at the front of the cell

is balanced by a concentric cortical/peripheral distribution of forces, which together with the circular cell contour at the rear of the cell is consistent with a possible hydrostatic loading (turgor pressure) of the cytoskeleton. The (+) configuration of Mode 3 is characterized by a more concentrated spot of traction stresses at the back of the cell, especially for *wt* cells. Mode 4 is an asymmetrical mode in which the cell adopts an S-shape (it bends twice in opposite directions) and it is associated with an imbalance of lateral forces.

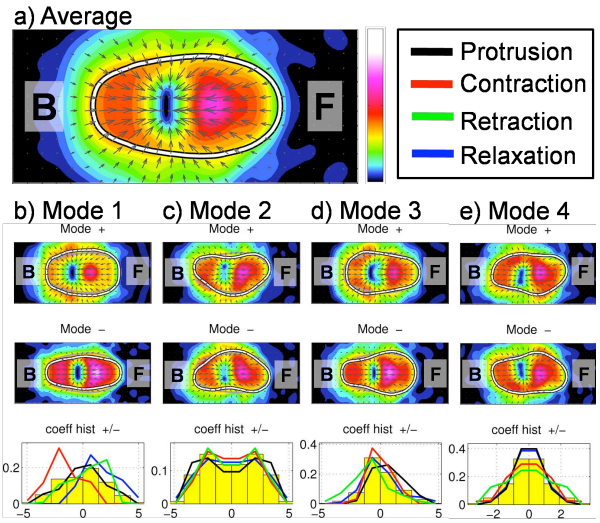

Figure 7. PCA of the shape and traction forces of a migrating *mlcE-Dictyostelium* cell.

VI. Relevance of the PCA modes

A comparison of the importance of the four most relevant PCA modes during the stages of the motility cycle of three cell lines of *Dictyostelium* cells (*wt*, *mhcA*- and *mlcE*-) is shown in Figure 8. The data indicates that Modes 2 and 4 are substantially less important in *mhcA*- cells than in the other two strains, indicating that purely frontal protrusion is more dominant over sideways protrusion for *mhcA*- cells, whereas the opposite holds for *wt* and *mlcE*-. Sideways protrusion of pseudopods are associated with local enhancements of lateral tension and cortical F-actin at one side of the cell, which is required to balance the internal torque produced on the actin cytoskeleton. Otherwise the protruding pseudopod could not be mechanically stable. The implication is that *mhcA*- cells are less effective in controlling their lateral tension and therefore have impaired sideways protrusion. This defect may explain the reduced frequency of pseudopod protrusion in *mhcA*- cells, which was observed by Wessels *et al* [3]. Consistent with these ideas, Fukui *et al* [10] reported reduced stability of protruding pseudopodia in *mhcA*- cells subjected to centrifugal forces.

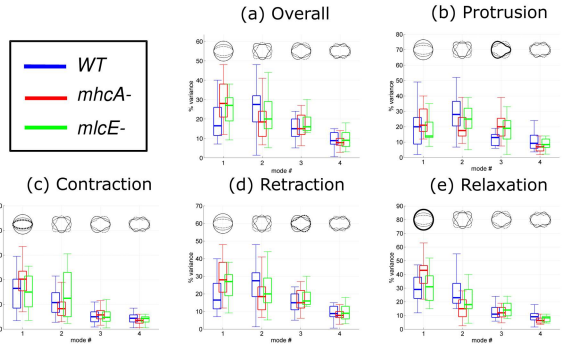

Figure 8: Box plots of the percentage of cell shape variance associated to each of the four principal modes for *wt* (blue, N=23 cells), *mhcA*-(red, N =22 cells) and *mlcE*- (green, N=15). (a) during the overall motion of the cells; (b) during protrusion; (c) during contraction; (d) during retraction; (e), during relaxation. The cell shape variance contained in each mode is determined from the histograms of the weight factors (examples of those are presented for *wt*, *mhcA*- and *mlcE*- cells in Figures 5-7).

References

[1] Lauffenburger, D.A., and Horwitz, A.F.: 'Cell migration: a physically integrated molecular process', Cell, 1996, 84, (3), pp. 359-369

[2] Ausprunk, D.H., and Folkman, J.: 'Migration and Proliferation of Endothelial Cells in Preformed and Newly Formed Blood-Vessels During Tumor Angiogenesis', Microvasc. Res., 1977, 14, (1), pp. 53-65

[3] Wessels, D., Soll, D.R., Knecht, D., Loomis, W.F., De Lozanne, A., and Spudich, J.A.: 'Cell motility and chemotaxis in Dictyostelium amebae lacking myosin heavy chain', Dev. Biol., 1988, 128, (1), pp. 164-177

[4] del Alamo, J., Meili, R., Alonso-Latorre, B., Rodriguez-Rodriguez, J., Aliseda, A., Firtel, R., and Lasheras, J.: 'Spatio-temporal analysis of eukaryotic cell motility by improved force cytometry', Proc. Natl. Acad. Sci. U.S.A., 2007, 104, (33), pp. 13343-13348

[5] Uchida, K.S., Kitanishi-Yumura, T., and Yumura, S.: 'Myosin II contributes to the posterior contraction and the anterior extension during the retraction phase in migrating Dictyostelium cells', J. Cell Biol., 2003, 116, (Pt 1), pp. 51-60

[6] Dembo, M., Oliver, T., Ishihara, A., and Jacobson, K.: 'Imaging the traction stresses exerted by locomoting cells with the elastic substratum method', Biophys. J., 1996, 70, (4), pp. 2008-2022

[7] Berkooz, G., Holmes, P., and Lumley, J.: 'The Proper Orthogonal Decomposition in the Analysis of Turbulent Flows', Ann. Rev. Fluid Mech., 1993, 25, pp. 539-575

[8] Killich, T., Plath, P., Hass, E., Xiang, W., Bultmann, H., Rensing, L., and Vicker, M.: 'Cell-movement and shape are nonrandom and determined by intracellular, oscillatory rotating waves in Dictyostelium amebas', Biosystems, 1994, 33, (2), pp. 75-87

[9] Keren, K., Pincus, Z., Allen, G., Barnhart, E., Marriott, G., Mogilner, A., and Theriot, J.: 'Mechanism of shape determination in motile cells', Nature, 2008, 453, (7194), pp. 475-U471

[10] Fukui, Y., Uyeda, T., Kitayama, C., and Inoué, S.: 'How well can an amoeba climb?', Proc. Natl. Acad. Sci. U.S.A., 2000, 97, (18), pp. 10020-10025